Selection rules for ring currents in radial π systems: trannulene substructures in hydrogenated fullerene cages

Remco W. A. Havenith,[a] André Rassat[b] and Patrick W. Fowler *[a]

[a] *School of Chemistry, University of Exeter, Stocker Road, Exeter, UK EX4 4QD. E-mail: P.W.Fowler@exeter.ac.uk; Fax: +44-1392-263434*
[b] *École Normale Supérieure and CNRS, 24 rue Lhomond, F75231 Paris Cedex 05, France. E-mail: andre.rassat@ens.fr; Fax: +33-144323325*

Received (in Cambridge, UK) 18th December 2001, Accepted 1st February 2002
First published as an Advance Article on the web 20th February 2002

Maps of induced current density are computed with the coupled Hartree–Fock, distributed-gauge, CTOCD-DZ method for the trannulene isomers of the hydrogenated fullerenes $C_{20}H_{10}$ and $C_{24}H_{12}$. Orbital analysis identifies 'in-plane' ring currents in trannulenes that obey equivalent selection rules to those for conventional annulenes. Thus, in systems of either type, 4-electron diatropicity is associated with electron counts of $4n + 2$, 2-electron paratropicity with $4n$.

Introduction

Orbital models explain the link between aromaticity and electron-count in π systems.[1] For example, it can be shown that the characteristic diatropic ring current of the $4n + 2$ aromatic monocycle arises entirely from the HOMO ⟶ LUMO transition.[2] Similarly, the paratropic ring current of a (planarised[3]) $4n$ monocycle is dominated by the Jahn–Teller-split HOMO ⟶ LUMO excitation.[2] Both conclusions rely on simple angular-momentum and symmetry arguments applied to the ipsocentric distributed-gauge formulation of magnetic-field-induced current density. The underlying orbital model has also been successfully applied to a number of substituted and polycyclic systems.[1,4,5]

Aromaticity is, however, not confined to conventional π systems on planar frameworks. In-plane aromaticity, for example, has been inferred in many molecules with unconventional topologies such as those of the [*n*]trannulene family.[6] Trannulenes are formally obtained by wrapping an *all-trans* cyclic polyene onto a cylinder. The resulting overlap of adjacent radial p orbitals can result in in-plane analogues of conventional aromatic and anti-aromatic systems.[6,7] Simple $(CH)_n$ trannulenes have been found to occupy minima, albeit high-lying, on the potential energy surface.[6] One route to their stabilisation is *via* the functionalisation of fullerenes,[8] where an unsaturated trannulene substructure on the carbon framework may emerge as part of an addition pattern.

In the present paper, the orbital model is used to derive selection rules for the ring currents in trannulenes. It will be shown that the same arguments, expressed in the different point groups appropriate to the two situations, can account for both conventional and radial 'in-plane' aromaticity of monocycles. We consider the [10]- and [12]trannulenes that would be formed by hydrogenating all but the equatorial belts of the two smallest possible fullerene cages C_{20} and C_{24}. Ring-current calculations on these "trapped trannulenes" are used to derive insights into the expected[6] variation of aromaticity within the whole family.

Computational results

Structures

$C_{20}H_{10}$ (**1**, D_{5d}, Fig. 1) and $C_{24}H_{12}$ (**2**, D_6) represent $4n + 2$ and $4n$ trannulenes with $n = 2$ and 3, respectively. Their structures were optimised at the RHF/6-31G** level (GAMESS-UK[9]) and confirmed as minima by diagonalisation of the Hessian matrix. Compound **1** retains full D_{5d} symmetry[6,7] whereas **2** distorts from its formal maximum symmetry point group of D_{6d} to D_6, corresponding to significant bond alternation in the equatorial belt. Ellipsoidal distortion of the dodecahedron in **1** is reflected in the different radial distances of polar and equatorial carbon atoms from the centre of mass: R(polar) = 2.232 Å and R(equatorial) = 1.939 Å.

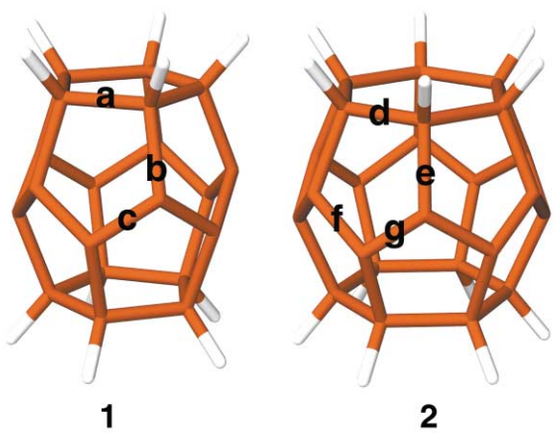

Fig. 1 Geometric structures of **1** and **2**, optimised at the RHF/6-31G** level, showing lengths and angles of salient bonds. $a = 1.571$, $b = 1.532$, $c = 1.384$, $d = 1.591$, $e = 1.540$, $f = 1.440$, and $g = 1.320$ Å. $\angle bc = 113.1°$, $\angle cc' = 107.9°$, $\angle ef = 111.9°$, $\angle eg = 115.0°$ and $\angle fg = 108.7°$.

The computed valence electronic configurations of **1** and **2** are

$$[(3a_{1g})^2(3e_{1u})^4(3a_{2u})^2(4a_{1g})^2(3e_{2g})^4(3e_{1g})^4(4e_{1u})^4(3e_{2u})^4(4e_{2u})^4(4a_{2u})^2\text{-}(4e_{2g})^4(5a_{1g})^2(5a_{2u})^2(4e_{1g})^4(5e_{1g})^4(5e_{1u})^4(5e_{2u})^4(6a_{1g})^2(5e_{2g})^4(6e_{1g})^4\text{-}(7a_{1g})^2(1a_{1u})^2(6e_{1u})^4(6e_{2u})^4(6e_{2g})^4(7e_{1u})^4(7e_{2g})^4]$$

and

$$[(3a_1)^2(5e_1)^4(3a_2)^2(5e_2)^4(6e_1)^4(4a_1)^2(3b_2)^2(7e_1)^4(6e_2)^4(3b_1)^2(7e_2)^4\text{-}(4a_2)^2(8e_2)^4(4b_1)^2(4b_2)^2(5a_1)^2(8e_1)^4(5a_2)^2(9e_1)^4(9e_2)^4(10e_1)^4(5b_2)^2\text{-}(5b_1)^2(6a_1)^2(11e_1)^4(10e_2)^4(7a_1)^2(6b_1)^2(12e_1)^4(11e_2)^4(6b_2)^2(8a_1)^2\text{-}(12e_2)^4(13e_1)^4(13e_2)^4(7b_2)^2],$$

This journal is © The Royal Society of Chemistry 2002

respectively. The lowest unoccupied molecular orbitals of **1** and **2** are of e_{2u} and b_1 symmetry, respectively. The orbital energies from these RHF/6-31G** calculations are: ε(HOMO, **1**) = −0.2504 E_h, ε(LUMO, **1**) = 0.0940 E_h, ε(HOMO, **2**) = −0.2239 E_h and ε(LUMO, **2**) = 0.0542 E_h.

Bonding in these trannulenes can be described in terms of radial and tangential molecular orbitals:[10] an 'in-plane π system' is superimposed on the edge-bonding σ framework of the polyhedral carbon cage. To a first approximation, the π system is made up of radially directed p orbitals on the 'equatorial' carbon sites, which span a cyclic Hückel-like system. As in the standard description of fullerenes,[11] the rôle of the tangential p orbitals is then to contribute to the σ framework of bonds along edges of the polyhedron. Radial–tangential separation is not rigorously enforced by symmetry in these curved systems, but it still provides a convenient approximate language and accurately represents the composition of the frontier orbitals.

In detail, C–H bonds account for the symmetries

$$\Gamma(\mathrm{CH}, \mathbf{1}) = a_{1g} + e_{1g} + e_{2g} + a_{2u} + e_{1u} + e_{2u}$$

and

$$\Gamma(\mathrm{CH}, \mathbf{2}) = a_1 + a_2 + b_1 + b_2 + 2e_1 + 2e_2.$$

The full σ framework of the polyhedral carbon cage is spanned by occupied edge-bonding orbitals of symmetries

$$\Gamma(\mathrm{frame}, \mathbf{1}) = 3a_{1g} + 3e_{1g} + 3e_{2g} + 1a_{1u} + 2a_{2u} + 3e_{1u} + 3e_{2u}$$

and

$$\Gamma(\mathrm{frame}, \mathbf{2}) = 4a_1 + 2a_2 + 3b_1 + 3b_2 + 6e_1 + 6e_2.$$

The radial p orbitals of the equatorial sites span symmetries Γ(radial, **1**) = Γ(CH, **1**) and Γ(radial, **2**) = Γ(CH, **2**); these dominate the bonding orbitals $7a_{1g}$, $7e_{1u}$ and $7e_{2g}$ of **1** and $7a_1$, $13e_1$, $13e_2$ and $7b_2$ of **2**, respectively. The pairs of tangential p orbitals on the equatorial sites span

$$\Gamma(\mathrm{tangential}, \mathbf{1}) = 2(a_{2g} + e_{1g} + e_{2g} + a_{1u} + e_{1u} + e_{2u})$$

and

$$\Gamma(\mathrm{tangential}, \mathbf{2}) = 2(a_1 + a_2 + b_1 + b_2 + 2e_1 + 2e_2),$$

respectively, and contribute to edge-bonding orbitals.

Current-density maps

The aromatic character of **1** and **2** can be assessed directly by computing ring-current maps, using a technique such as the CTOCD-DZ method,[12,13] which is implemented in the SYSMO program.[14] For a planar π system, the current density induced by a perpendicular magnetic field is usually plotted in a plane parallel to that of the molecule, and at a height of 1 a_0.[15] Here, in order to capture the three-dimensional nature of the π system, we present plots drawn in two different planes. The first is the equatorial plane of the molecule. The second is a perpendicular tangential plane, perpendicular to a radius drawn through the midpoint of a formal double bond of the trannulene ring and lying at a distance of 1 a_0 from that point. In both cases, the magnetic field is directed parallel to the principal symmetry axis, and current vectors are projected into the given plotting plane.

Total current-density maps for **1** and **2**, plotted in the equatorial plane, are presented in Figs. 2 and 3. The current density has a large variation in intensity associated with the fact that the plotting plane in this case cuts through framework bonds. The maps are therefore shown in two versions: (a) 'scaled', where arrow length and width are proportional to the in-plane component of current density, and (b) 'unscaled', where all arrows are of equal length. The scaled map allows direct comparison of intensity, but the unscaled map shows more clearly the overall pattern of circulation.

For **1**, working outwards from the centre of the map, the main features are (i) a weak internal paratropic circulation around the void, (ii) a stronger diatropic circulation on the surface of the carbon framework, (iii) strong local paratropic circulations in the cut bonds and, finally, (iv) the external diatropic circulation found for all closed-shell molecules. For **2**, the innermost region of the map is similar to that of **1**, but the framework circulation (ii) is now strong and *paratropic*, and the paratropic circulations in the cut bonds (iii) are stronger, leading to some perturbation of the outermost global diatropic region (iv).

The source of the differences in pattern between the two molecules can be understood by partitioning the total current density into orbital contributions.[1] The dominant orbital contributions are therefore also included in Figs. 2 and 3. In each molecule the framework ring current (ii) is attributable solely to the HOMO contribution. In **1** the four electrons of an e_{2g} HOMO give rise to the diatropic circulation and in **2** the two electrons of the b_2 HOMO give rise to the paratropic circulation in the same region. The plots in the tangential plane show that these ring currents are corrugated, following the zig-zag of the trannulene cycle (Figs. 2f and 3f).

The set of localised paratropic cut-bond circulations (iii) in **1** and **2** is also attributable to a particular orbital: to the combination of tangential p orbitals that consists of positive and negative σ-bonding lobes on alternate equatorial edges. The plots in the tangential plane show that the flow in the cut bonds runs parallel to the molecular equator in both cases (Figs. 2d and 3d).

Thus, the essential difference between the two systems is that the $(4n + 2)$ trannulene **1** has a HOMO-dominated diatropic ring current whereas the $4n$ trannulene **2** has a HOMO-dominated paratropic ring current. The sense of these currents is compatible with the reported NICS[16] values for the corresponding isolated trannulenes (−14.0 for [10]- and 35.7 ppm for [12]trannulene, respectively[6]), and matches simple expectations based on aromatic and anti-aromatic electron counts.

Discussion

The fact that trannulenes obey the same rules for currents as conventional Hückel monocycles follows directly from the orbital picture of the origin of the ring currents in these systems. In CTOCD, the first-order wavefunction can be written as a sum over transitions from occupied molecular orbitals,[1] and this form gives rise to symmetry-based selection rules. The key symmetries are those of the angular momentum operator describing rotation about the magnetic field direction, and yielding paramagnetic contributions, and the linear momentum operators describing translations in the plane perpendicular to the magnetic field, and giving rise to diamagnetic contributions.[1,2] Transitions are strictly from occupied to virtual orbitals, and the operator matrix elements are modulated by energy denominators, which favour orbitals near the molecular Fermi level.

In a conventional Hückel $4n + 2$ system, the only allowed occupied-to-virtual transition is from the HOMO to LUMO, and this is translationally allowed, thus producing the characteristic diamagnetic current.[2] In the corresponding $4n + 2$ trannulene, the symmetry labels of the 'in-plane π system' now follow $D_{(2n+1)d}$ rather than $D_{(4n+2)h}$ symmetry. Thus in **1**, the HOMO–LUMO transition is $7e_{2g} \longrightarrow 7e_{2u}$ (Scheme 1). In $D_{(2n+1)d}$ symmetry, however, this remains the sole allowed occupied-to-virtual translational transition in the 'π' space of **1**. Diatropic ring currents are thus expected and are found.

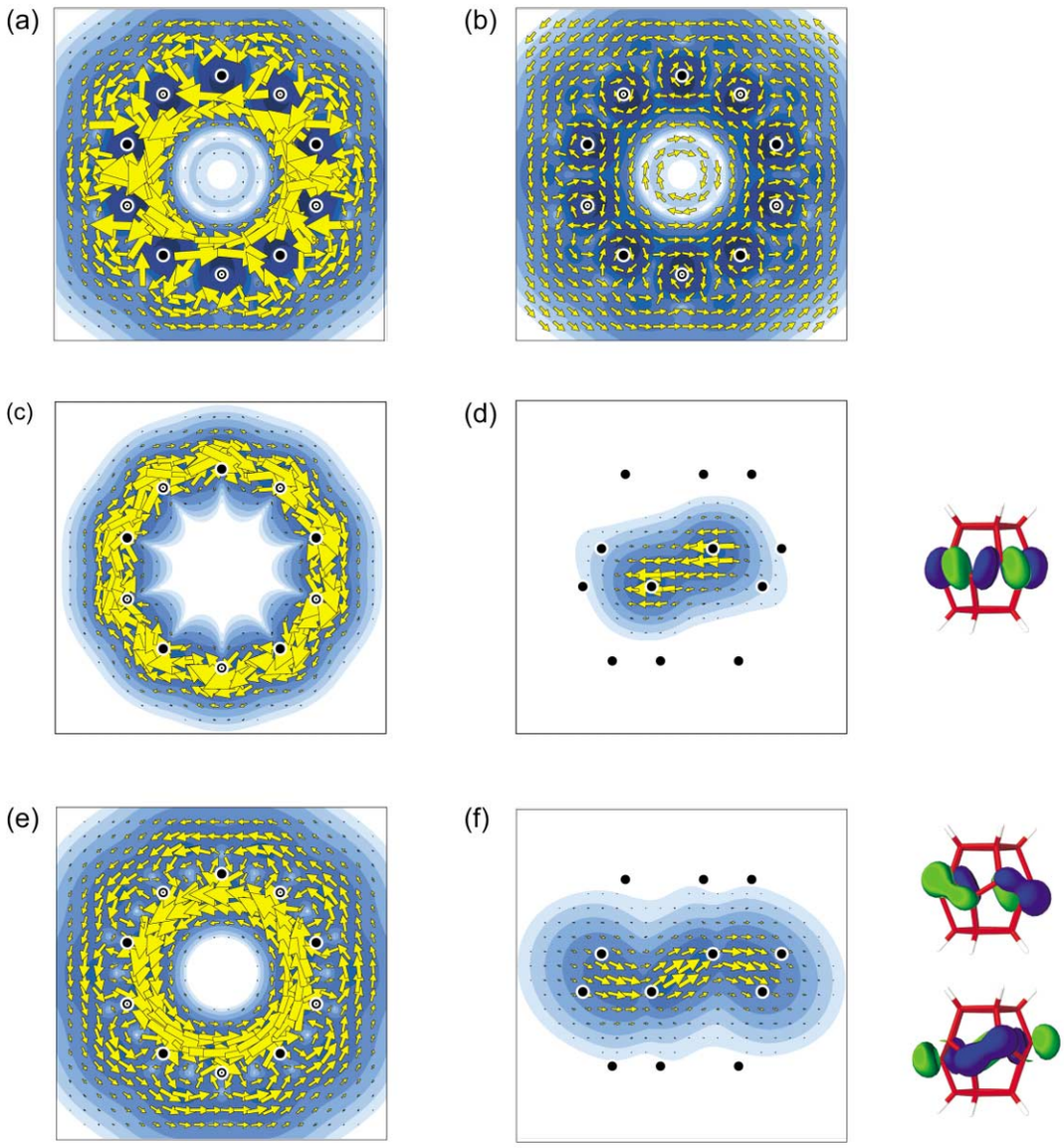

Fig. 2 Current-density maps for **1**. (a) Total 'scaled' and (b) total 'unscaled' current densities in the equatorial plane; the contribution of the $1a_{1u}$ edge-bonding orbital in (c) the equatorial and (d) the tangential planes; the contribution of the $7e_{2g}$ in-plane π orbital in (e) the equatorial and (f) the tangential planes. The contours denote the modulus of the current density and vectors represent its in-plane projection. Diamagnetic (diatropic) circulation is shown anti-clockwise/left to right and paramagnetic (paratropic) circulation clockwise/right to left. In (a), (b), (c) and (e), near-equatorial carbon centres are shown as ● (above) and ☉ (below); in (d) and (f) all carbon centres are indicated.

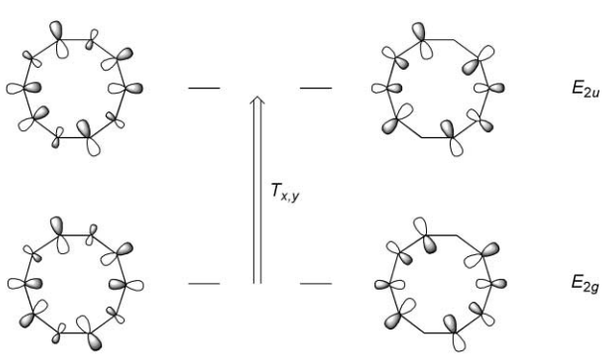

Scheme 1 HOMO–LUMO transition for the $(4n + 2)$-electron in-plane aromatic trannulene $C_{20}H_{10}$ (**1**). $T_{x,y}$ represents a translation in the equatorial plane.

A similar transposition can be applied to the anti-aromatic systems. For a (planarised [3]) $4n$ system, the HOMO and LUMO would be degenerate in the high D_{4nh} symmetry of the equilateral monocycle, but they are split by a Jahn–Teller distortion that results in a bond-alternated system with D_{2nh} symmetry. The dominant transition is then the low-energy, rotationally allowed HOMO ⟶ LUMO excitation between the components of the split pair.[2] This result carries over directly to the [$4n$]trannulenes. The equilateral trannulene would have D_{2nd} symmetry, which is lowered by Jahn–Teller distortion to D_{2n}. In **2**, the $7b_2 \longrightarrow 7b_1$ HOMO–LUMO transition is then rotationally allowed (Scheme 2) and hence gives rise to an intense paratropic ring current.

In addition to the ring currents, the orbital picture also accounts for the paratropic nature of the local σ-bond contributions to the total current-density map. A concerted local rotation of the tangential p orbitals transforms the active σ orbital with its alternating phase on neighbouring edges into a low-lying, anti-bonding, in-plane, radial π orbital [**1**: $1a_{1u}$ (HOMO − 5) ⟶ $6a_{2u}$ (LUMO + 1); **2**: $8a_1$ (HOMO − 4) ⟶ $6a_2$ (LUMO + 2), Scheme 3]. Thus, the paramagnetic sense of this cut-bond current, seen in the equatorial-plane maps, also follows from the selection rules.

Conclusion

Analysis of *ab initio* current-density maps allows a unified picture of magnetically defined aromaticity in conventional and

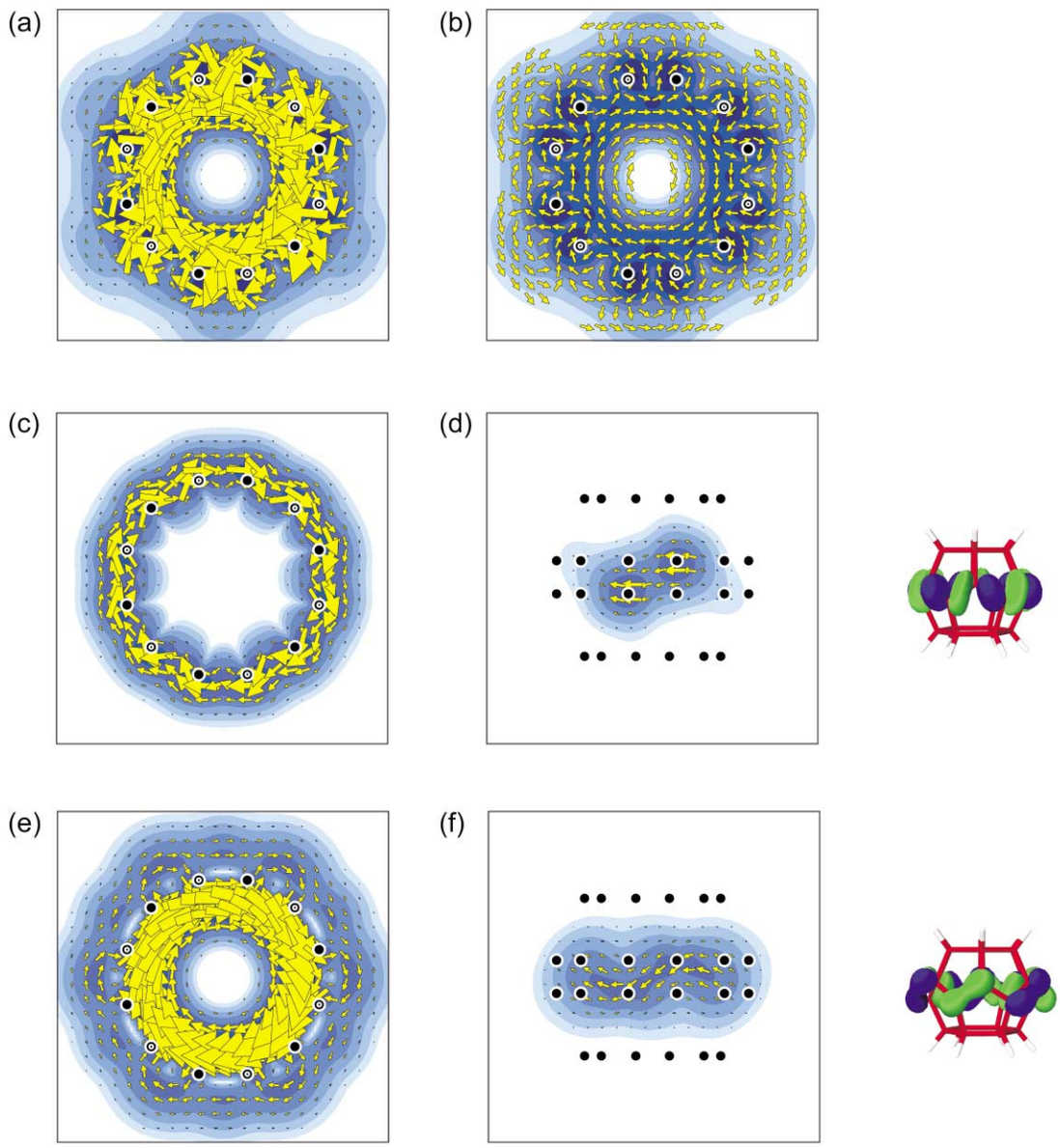

Fig. 3 Current-density maps for **2**. (a) Total 'scaled' and (b) total 'unscaled' current densities in the equatorial plane; the contribution of the $8a_1$ edge-bonding orbital in (c) the equatorial and (d) the tangential planes; the contribution of the $7b_2$ in-plane π orbital in (e) the equatorial and (f) the tangential planes. Plotting details as in Fig. 2.

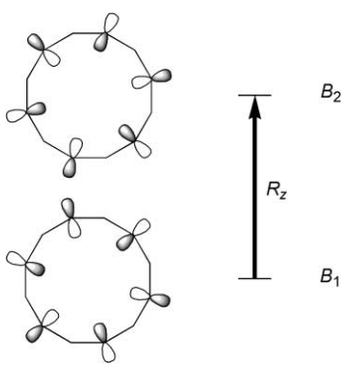

Scheme 2 HOMO–LUMO transition for the 4*n*-electron in-plane anti-aromatic trannulene $C_{24}H_{12}$ (**2**). R_z represents a rotation about the principal axis.

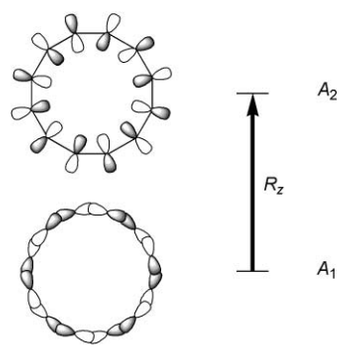

Scheme 3 Rotationally allowed transition from an edge-bonding to a π* orbital in $C_{24}H_{12}$ (**2**). R_z here represents a concerted rotation on all sites.

in-plane π systems. Crucially, the ipsocentric CTOCD-DZ method combines numerical accuracy with transparency of interpretation in terms of orbital contributions. Differences between in- and out-of-plane orientations of the contributing p orbitals lead to changes in group theoretical labels, but in both cases 4-electron diatropicity is found at electron counts of $4n + 2$, and 2-electron paratropicity at $4n$. Hence, the orbital picture gives the explanation for the observation based on calculated geometries and magnetic properties of $(CH)_n$ trannulenes ($10 \leq n \leq 30$)[6] that the [*n*]trannulenes obey the conventional annulene Hückel rule exactly.

Acknowledgements

Dr E. Steiner is thanked for many helpful discussions on the theory of ring currents. We thank the European Union TMR scheme, contract FMRX-CT097-0192 (BIOFULLERENES) and the Royal Society of Chemistry International Author Scheme for financial support.

References

1 E. Steiner and P. W. Fowler, *J. Phys. Chem. A*, 2001, **105**, 9553.
2 E. Steiner and P. W. Fowler, *Chem. Commun.*, 2001, 2220.
3 A. Matsuura and K. Komatsu, *J. Am. Chem. Soc.*, 2001, **123**, 1768.
4 E. Steiner and P. W. Fowler, *ChemPhysChem*, 2002, **3**, 114.
5 R. W. A. Havenith, P. W. Fowler and E. Steiner, *J. Chem. Soc., Perkin Trans. 2*, 2002, 502
6 A. A. Fokin, H. Jiao and P. von R. Schleyer, *J. Am. Chem. Soc.*, 1998, **120**, 9364.
7 A. B. McEwen and P. von R. Schleyer, *J. Org. Chem.*, 1986, **51**, 4357.
8 X.-W. Wei, A. D. Darwish, O. V. Boltalina, P. B. Hitchcock, J. M. Street and R. Taylor, *Angew. Chem.*, 2001, **113**, 3077; X.-W. Wei, A. D. Darwish, O. V. Boltalina, P. B. Hitchcock, J. M. Street and R. Taylor, *Angew. Chem., Int. Ed.*, 2001, **40**, 2989.
9 M. F. Guest, J. H. van Lenthe, J. Kendrick, K. Schöffel, P. Sherwood and R. J. Harrison, *GAMESS-UK, a package of ab initio programs*, 2000. With contributions from: R. D. Amos, R. J. Buenker, H. J. J. van Dam, M. Dupuis, N. C. Handy, I. H. Hillier, P. J. Knowles, V. Bonačić-Koutecký, W. von Niessen, R. J. Harrison, A. P. Rendell, V. R. Saunders, A. J. Stone, D. J. Tozer and A. H. de Vries. It is derived from the original GAMESS code due to: M. Dupuis, D. Spangler and J. Wendolowski, *NRCC Software Catalog, Program No. QG01 (GAMESS)*, 1980, vol. 1.
10 A. J. Stone, *Mol. Phys.*, 1980, **41**, 1339.
11 P. W. Fowler and J. Woolrich, *Chem. Phys. Lett.*, 1986, **127**, 78.
12 T. A. Keith and R. F. W. Bader, *Chem. Phys. Lett.*, 1993, **210**, 223.
13 R. Zanasi, *J. Chem. Phys.*, 1996, **105**, 1460.
14 P. Lazzeretti and R. Zanasi, *SYSMO package*, University of Modena, 1980. Additional routines for evaluation and plotting of current density: E. Steiner and P. W. Fowler.
15 E. Steiner, P. W. Fowler and L. W. Jenneskens, *Angew. Chem.*, 2001, **113**, 375; E. Steiner, P. W. Fowler and L. W. Jenneskens, *Angew. Chem., Int. Ed.*, 2001, **40**, 362.
16 P. von R. Schleyer, C. Maerker, A. Dransfeld, H. Jiao and N. J. R. van Eikema Hommes, *J. Am. Chem. Soc.*, 1996, **118**, 6317.